

Cellular Characterization of the Gouty Tophus

A Quantitative Analysis

Nicola Dalbeth, Bregina Pool, Greg D. Gamble, Timothy Smith, Karen E. Callon, Fiona M. McQueen, and Jillian Cornish

Objective. To characterize the cellular architecture of the tophus and to determine the presence of cytokines implicated in the initiation and resolution of gouty inflammation.

Methods. Sixteen fixed, paraffin-embedded, uninfected tophus samples were surgically obtained from 12 patients with microscopically proven gout and were analyzed by quantitative immunohistochemistry. The number of cells present in the corona and fibrovascular zones of the tophus was analyzed by Genmod mixed models analysis.

Results. Numerous CD68+ mononucleated and multinucleated cells were present within the corona zone. Mast cells were identified in all tophus samples and at similar densities throughout the corona and fibrovascular zones. In contrast, neutrophils were rarely observed. Plasma cells were present in very high numbers within the corona zone. The overall number of CD20+ B cells was much lower. However, in 6 of 12 patients (50%), at least 1 B cell aggregate was present in the fibrovascular zone. Large numbers of cells expressing interleukin-1 β (IL-1 β) were observed in the corona zone. Transforming growth factor β 1 (TGF β 1)-expressing mononucleated cells were also identified. The number of CD68+ cells correlated with the number

of cells expressing IL-1 β ($r = 0.691$, $P = 0.009$) and the number expressing TGF β 1 ($r = 0.518$, $P = 0.04$).

Conclusion. The tophus represents a complex and organized chronic inflammatory tissue response to monosodium urate monohydrate crystals involving both innate and adaptive immune cells. The coexpression of IL-1 β and TGF β 1 suggests that both proinflammatory and antiinflammatory factors present within the tophus contribute to a cycle of chronic inflammation, attempted resolution, and tissue remodeling.

Acute gout is characterized by an intense self-limiting inflammatory response with infiltration of neutrophils into the synovial membrane and synovial fluid (1). The mechanisms of acute gouty inflammation have been extensively studied (for review, see ref. 2). Recent studies have identified the pivotal role of the innate immune response, in particular, NALP3 inflammasome activation and interleukin-1 β (IL-1 β) release from mononuclear phagosomes, in the initiation phase of acute gout (3,4). The resolution phase of acute gout may be mediated by a number of factors but especially by macrophage differentiation and production of transforming growth factor β 1 (TGF β 1) (5–7).

In the presence of persistent hyperuricemia, some patients also develop chronic gout. The gouty tophus is the hallmark of chronic gout. This lesion typically occurs within subcutaneous tissues and within the joints. Tophi are usually nontender, but they may lead to cosmetic problems, mechanical obstruction of joint movement, and musculoskeletal disability (8). These lesions have also been implicated in the pathogenesis of joint damage in gout (9).

In contrast to acute gout, the characteristics and mechanisms of chronic gout have been much less intensively examined. Microscopically, tophi appear as chronic granulomatous lesions comprising collections of

Supported by a New Zealand Lottery Health Research Grant and by the Auckland Medical Research Foundation.

Nicola Dalbeth, MD, FRACP, Bregina Pool, BSc (Hons), Greg D. Gamble, MSc, Timothy Smith, MSc, Karen E. Callon, BSc, Fiona M. McQueen, MD, Jillian Cornish, PhD: University of Auckland, Auckland, New Zealand.

Address correspondence and reprint requests to Nicola Dalbeth, MD, FRACP, Bone Research Group, Department of Medicine, Faculty of Medical and Health Sciences, University of Auckland, 85 Park Road, Grafton, Auckland, New Zealand. E-mail: n.dalbeth@auckland.ac.nz.

Submitted for publication June 29, 2009; accepted in revised form January 11, 2010.

mononucleated and multinucleated macrophages surrounding a core of monosodium urate monohydrate (MSU) crystals and encased by dense connective tissue (1,10,11). Various zones have been identified within the tophus: the central crystalline core, the cellular corona zone surrounding the central core, and the outer fibrovascular zone (10).

Although several studies have examined the characteristics of macrophages within the gouty tophus (10,11), the cellular characteristics of the gouty tophus remain poorly defined. Such information is required for an understanding of the mechanisms and potential mediators of tophus formation. The aim of the present study was to characterize the cellular architecture of the tophus and to determine the presence of cytokines implicated in the initiation and resolution of gouty inflammation.

PATIENTS AND METHODS

Patients and samples. This study was approved by the local (Northern X) ethics committee, and all patients provided written informed consent. Sixteen fixed, paraffin-embedded tophus samples were obtained from 12 patients who underwent surgery for removal of tophi. Clinical details were obtained by chart review. All patients had microscopically proven gout. Patients with gout who were undergoing surgery for infected tophi were not included in the study.

Immunohistochemistry. Tophus samples were fixed in neutral buffered formalin and embedded in paraffin. Consecutive 4μ sections were made 150μ apart and were mounted on Superfrost glass slides. After dewaxing with Safsolvent (Ajax Chemicals), slides were rehydrated through graded ethanol solutions. Once hydrated, sections were microwave heated for 30 minutes at 96°C in Dako Target Retrieval Solution (pH 6.0 for CD20, TGF β 1, and tartrate-resistant acid phosphatase [TRAP] and pH 9.0 for CD3, CD8, CD68, plasma cell, mast cell tryptase, and IL-1 β ; no antigen retrieval was required for neutrophil elastase). For all antibodies except anti-IL-1 β , an EnVision Plus Dual Link System-HRP kit containing dual endogenous enzyme block, peroxidase-labeled polymer conjugated to goat anti-mouse/rabbit IgG, buffered substrate, and diaminobenzidine (DAB+) chromogen was used (all from Dako).

To each slide, 10% goat serum (Sigma) was added in phosphate buffered saline (PBS) for 30 minutes, and following washing with PBS, the slides were incubated in dual endogenous enzyme block for 5 minutes. Slides were washed and then incubated with primary antibody or isotype control in PBS with 10% goat serum for 60 minutes at room temperature, except for CD3 and neutrophil elastase, which were incubated for 90 minutes, and TGF β 1, which was incubated overnight at 4°C in a humidified chamber. The following mouse anti-human primary antibodies and dilutions were used: anti-CD68 at a 1:50 dilution (clone PG-M1; Dako), anti-mast cell tryptase at a 1:100 dilution (clone AA1; Dako), anti-neutrophil elastase at a 1:25 dilution (clone NP57; Dako), anti-TRAP at a 1:100

dilution (clone ZY-9C5; Zymed), anti-CD3 at a 1:25 dilution (polyclonal rabbit; Dako), anti-plasma cell at a 1:50 dilution (clone VS38c; Dako), anti-CD8 at a 1:50 dilution (clone C8/144B; Dako), anti-CD20 at a 1:200 dilution (clone L26; Dako), and anti-TGF β 1 at a 1:50 dilution (polyclonal rabbit; Santa Cruz Biotechnology).

After washing in PBS, the slides were incubated for 60 minutes with peroxidase-labeled polymer-conjugated goat anti-mouse/rabbit IgG. Following further washes with PBS, the DAB+ solution was applied to the slides for 5 minutes. Slides were then washed with distilled water and weakly counterstained with hematoxylin for 25–30 seconds. Slides were then mounted with AquaMount (BDH) and analyzed by light microscopy.

In the case of IL-1 β staining, a rabbit ABC staining kit (Santa Cruz Biotechnology) was used. Following addition of blocking serum and peroxidase block, slides were incubated with anti-human IL-1 β polyclonal antibody at a 1:50 dilution (rabbit polyclonal) in PBS with 1.5% blocking serum for 90 minutes. Negative-staining control experiments were performed by using an isotype-matched polyclonal antibody. Sections were incubated for 30 minutes with a biotinylated secondary antibody and then with AB enzyme reagent for 30 minutes prior to application of DAB+ chromogen, counterstaining, and mounting as described above.

Quantification of staining results. In order to quantify the number of each cell type in various locations within the tophus, areas of the corona and fibrovascular zone were identified in each slide, as described by Palmer et al (10). For each cell type, 2 independent observers (BP and ND) completed all manual counting. Each observer counted the number of positively staining cells in each zone in 5 high-power fields throughout the slide at $20\times$ magnification (0.48 mm^2), and for each slide, the mean number of positively staining cells in each zone was recorded. In addition, the number of multinucleated CD68+ cells and multinucleated TRAP+ cells (osteoclast-like cells) was counted in a similar manner at each zone. The presence of B cell aggregates was also recorded within the entire slide. B cell aggregates were defined as areas of at least 20 adjacent cells with CD20+ staining. The observers were blinded to the clinical features as well as to the scores assigned by each other. The interobserver intraclass correlation coefficient for all markers in both zones was 0.865 (range 0.836–0.890). The scores for the 2 observers were averaged, and the average scores were used for analysis.

Statistical analysis. Medians with ranges and percentages were used to describe the clinical characteristics of participants. Genmod mixed models analysis was used for analysis of the location of the cells to account for repeated counts within the same person. The relationship between clinical features and the total number of cells was analyzed by Spearman's correlations and Wilcoxon's rank sum tests. The median counts for each cell type within the corona and fibrovascular zones were used to construct a cellular model of the tophus.

RESULTS

Clinical characteristics. We analyzed 16 surgical samples of tophi obtained from 12 patients with micro-

Table 1. Patient and tophus characteristics at the time of surgery

Patient characteristics (n = 12)	
No. (%) male	11 (92)
Age, median (range) years	55 (44–91)
Duration of gout, median (range) years	14 (1–30)
No. (%) prescribed allopurinol	6 (50)
No. (%) prescribed antiinflammatory agents*	6 (50)
Serum urate, median (range) mmoles/liter	0.44 (0.20–0.66)
Tophus characteristics (n = 16)	
Duration of tophus, median (range) years	4 (1.5–8)
No. (%) intraarticular tophi	7 (44)
No. (%) extraarticular tophi†	9 (56)
No. (%) tender	0 (0)
No. (%) enlarging or stable in size at time of excision	16 (100)
No. (%) reducing in size at time of excision	0 (0)

* Includes nonsteroidal antiinflammatory drugs and colchicine.

† Within the bursae (n = 6) and tendons (n = 3).

scopically proven gout. The clinical features of the patients and tophi are described in Table 1. Patients were predominantly male, with large variations in disease duration and serum urate levels. No patients were receiving IL-1 antagonists. The tophi were resected from the following sites: fingers (n = 6), elbows (n = 5), feet (n = 2), ankle (n = 1), and knees (n = 2). Both intraarticular and extraarticular tophi were examined. No tophi were tender at the time of excision, and all were enlarging or stable in size.

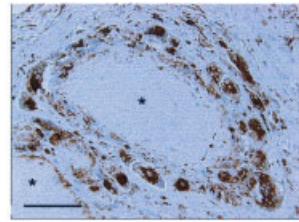
Cells of the innate immune system in gouty tophi.

Analysis of the tophus samples for macrophages confirmed the presence of numerous CD68+ cells within the corona zone (Figure 1 and Table 2). The majority of these cells were mononucleated, but multinucleated CD68+ cells were also identified adjacent to the central crystal core within the corona zone. Mononucleated CD68+ cells were present in lower numbers within the fibrovascular zone, and no multinucleated CD68+ cells were observed in this region (Table 2). As we have previously described (12), TRAP+ multinucleated cells (osteoclast-like cells) were also present within the corona zone (Table 2).

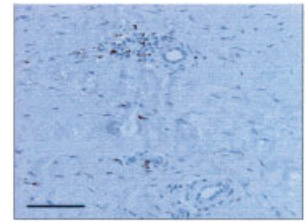
Mast cells were identified in all tophus samples (Figure 1 and Table 2). These cells were present throughout both the corona and fibrovascular zones at similar densities. In contrast, neutrophils were rarely observed in the samples. When present, these cells were more often observed in the corona zone (Figure 1 and Table 2).

Cells of the adaptive immune system in gouty tophi. CD8+ T cells were identified in both the corona and fibrovascular zones in all samples tested, although these cells were present at relatively low densities (Fig-

Macrophages (CD68)

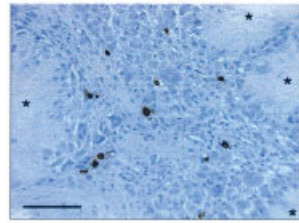


Corona zone

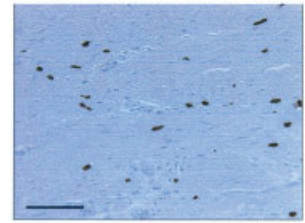


Fibrovascular zone

Mast cells

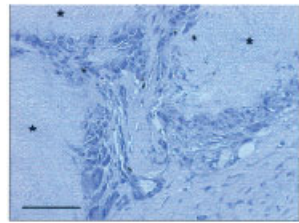


Corona zone

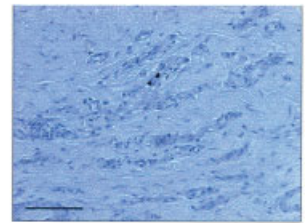


Fibrovascular zone

Neutrophils



Corona zone



Fibrovascular zone

Figure 1. Innate immune cells within the gouty tophus. Representative examples of staining for CD68+ cells, mast cells, and neutrophils within the corona and fibrovascular zones of the tophus are shown. Each asterisk marks the central core of a monosodium urate monohydrate crystal. Bars = 10 μ .

ure 2 and Table 2). Numerous plasma cells were present within the tophi (Figure 2). Of all cell types analyzed, the plasma cell densities within the corona zone were the highest recorded (Table 2). In contrast, the overall number of CD20+ B cells was much lower (Figure 2 and Table 2). In most areas, a few B cells were scattered throughout the corona and fibrovascular zones. However, in 8 samples from 6 of the 12 patients (50%), at least 1 B cell aggregate was present within the fibrovascular zone (Figure 2).

Cells expressing IL-1 β and TGF β 1 in gouty tophi. Large numbers of cells expressing IL-1 β were observed in the tophus samples. This was particularly apparent within the corona zone, both in mononucleated

Table 2. Summary of cell types in the corona and fibrovascular zones of tophi*

	Tophus zone		<i>P</i>
	Corona	Fibrovascular	
Cells of the innate immune system			
Macrophages (CD68)	50 (22.5–76.5)	10 (5–14)	<0.0001
CD68+ multinucleated cells	5 (3.5–19)	0 (0–0)	<0.0001
TRAP+ multinucleated cells	19 (8–29)	0 (0–0)	<0.0001
Mast cells	16 (10.5–24.5)	19 (11.5–24.5)	0.39
Neutrophils	0.5 (0–1.5)	0 (0–1.5)	0.00995
Cells of the adaptive immune system			
CD3+ T cells	14 (4–25)	11 (5–23)	0.40
CD8+ T cells	11 (8–42)	18 (5–40)	0.92
Plasma cells	64 (34.5–104)	15.5 (5–35)	<0.0001
CD20+ B cells	0 (0–2.0)	6 (3.5–12.5)	0.049
Cells expressing cytokines			
IL-1 β	155 (131–206)	21 (12–23)	<0.0001
TGF β 1	26.5 (17.5–36.5)	6.5 (3.5–12.5)	0.0088

* A total of 16 uninfected tophi obtained from 12 patients with microscopically proven gout were analyzed. Values are the median (interquartile range) number of cells per high-power field counted at 20 \times magnification. *P* values were determined by Genmod mixed models analysis for repeated counts within the same subject. TRAP = tartrate-resistant acid phosphatase; IL-1 β = interleukin-1 β ; TGF β 1 = transforming growth factor β 1.

and in multinucleated cells (Figure 3 and Table 2). Perivascular expression of IL-1 β was present in the fibrovascular zone. TGF β 1-expressing cells were also identified; these cells were typically mononucleated and were present at higher densities within the corona zone (Figure 3 and Table 2). Analysis of cytokine-producing cells within the corona showed that the number of CD68+ cells correlated with the number of cells expressing IL-1 β ($r = 0.691$, $P = 0.009$) and TGF β 1 ($r = 0.518$, $P = 0.04$).

Relationship between clinical features and cell counts in gouty tophi. There were no consistent differences in the extent of cellular infiltration according to the clinical characteristics shown in Table 1. In particular, intraarticular and extraarticular tophi had a similar pattern of distribution and a similar number of cells. The duration of tophi was inversely associated with the number of cells expressing IL-1 β ($r = -0.62$, $P = 0.04$).

DISCUSSION

The present study demonstrates that the tophus represents a complex and organized chronic inflammatory tissue response to MSU crystals. We found that both innate and adaptive immune cells are present in the gouty tophus, contrasting with the well-recognized, dominant role of innate immunity in the acute gout attack. The coexpression of IL-1 β and TGF β 1 within the tophus indicates that both proinflammatory and antiinflammatory factors present within the same lesion may contrib-

ute to a cycle of chronic inflammation, attempted resolution, and tissue remodeling.

Our analysis showed that a variety of cells are present within the tophus, and that the cellular architecture is consistent within different sites and different patients. These findings are summarized in the cellular model shown in Figure 4. Macrophages were present in large numbers, particularly in the corona zone adjacent to the central core of MSU crystals. Monocytes and macrophages have been strongly implicated in the initiation and resolution phases of acute gout (13,14), and our data support the concept that these cells also contribute to the development of the gouty tophus. Macrophage-derived factors that promote granuloma formation in response to MSU crystals are unknown. However, it is well recognized that IL-1 β is an important macrophage-derived cytokine that contributes to the formation of granulomas in other diseases, such as tuberculosis, rheumatoid arthritis, and parasitic infections (15–17), and it is likely that this cytokine plays a role in the formation of the gouty tophus. The inverse relationship between the duration of the tophus and the number of IL-1 β -producing cells observed in our study further supports this concept.

We also identified mast cells in all tophus samples, in both the corona and fibrovascular zones. This finding is of significance with regard to previous studies implicating endogenous mast cells in the development of the acute inflammatory response to MSU crystals in the

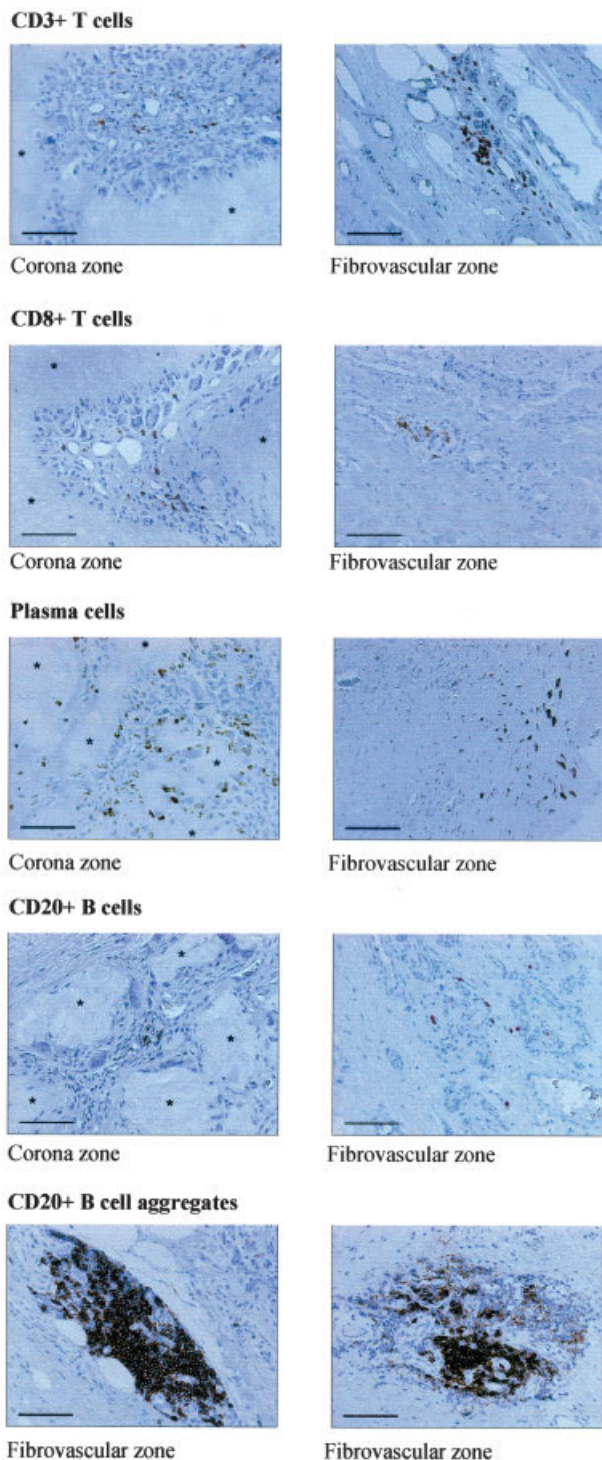


Figure 2. Adaptive immune cells within the gouty tophus. Representative examples of staining for CD3+ T cells, CD8+ T cells, plasma cells, and CD20+ B cells and B cell aggregates within the corona and fibrovascular zones of the tophus are shown. Each asterisk marks the central core of a monosodium urate monohydrate crystal. Bars = 10 μ .

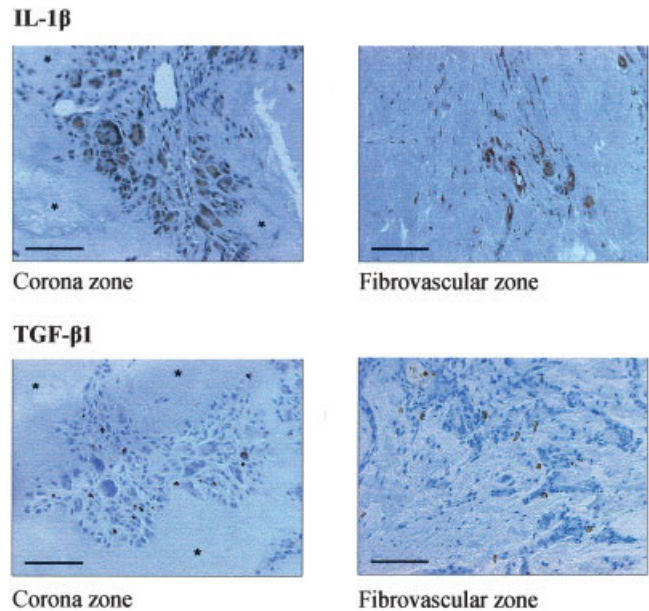


Figure 3. Cytokine expression within the gouty tophus. Representative examples of staining for interleukin-1 β (IL-1 β) and transforming growth factor β 1 (TGF β 1) within the corona and fibrovascular zones of the tophus are shown. Each asterisk marks the central core of a monosodium urate monohydrate crystal. Bars = 10 μ .

murine urate peritonitis model (18). Furthermore, mast cells have been identified in the subintimal layer of the MSU-injected pouch membrane soon after injection of MSU crystals in the rat air-pouch model (19). These cells have been implicated in development of inflammatory arthritis (20), and they promote fibroblast activation and proliferation, macrophage activation, cytokine expression (including IL-1 β and TGF β 1), angiogenesis, and osteoclast differentiation (for review, see ref. 21), all of which are features that are observed within the gouty tophus. Whether mast cells directly participate in the development of the gouty tophus is uncertain; *in vivo* studies modeling tophus formation are needed to address this question.

Our analysis of the cellular architecture of the tophus has implicated adaptive immunity in the development of these lesions. In particular, numerous plasma cells are present, predominantly in the corona zone. It is well recognized that MSU crystals are coated with immunoglobulins *in vivo*, and that this coating regulates the cellular responses to MSU crystals (22–25). Immunoglobulins (predominantly IgG and IgM) have been identified within the gouty tophus (22). Immunoglobulins (particularly IgM) also contribute to MSU crystal formation (25,26). These observations, together with our

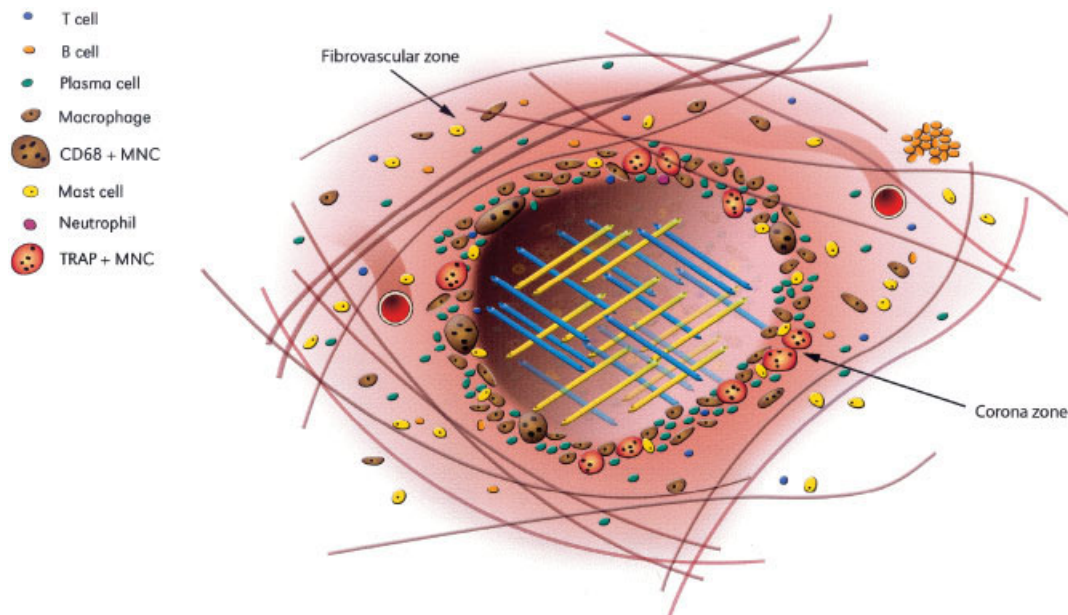


Figure 4. A cellular model of the gouty tophus. Cells are depicted in the corona and fibrovascular zones based on the type and number of cells identified by quantitative immunohistochemistry. MNC = mononuclear cells; TRAP = tartrate-resistant acid phosphatase.

finding that numerous plasma cells are located adjacent to the central core of the MSU crystal in the tophus, suggest that these cells contribute directly to both crystal formation and coordination of the cellular response within the tophus. The distribution of plasma cells within the tophus contrasts with the observed distribution of B cells. The presence of B cell aggregates within the fibrovascular zone in some tophi is reminiscent of the B cell aggregates present within the synovium and bone marrow in some patients with rheumatoid arthritis (27,28) and further implicates adaptive immunity in the formation of the gouty tophus. The functional relevance and factors contributing to the development of these aggregates in the gouty tophus are unknown.

The expression of IL-1 β within the tophus is particularly interesting in light of the pivotal role of this cytokine in the initiation phase of the acute gout attack. Our data indicate that this cytokine is expressed by large numbers of cells within the tophus, which is perhaps surprising given the apparent lack of overt clinical features of inflammation (such as tenderness, erythema, or heat) within most tophi. The paucity of neutrophils within the tophus may explain some of these findings, considering the importance of neutrophil influx and activation in the “second-phase” perpetuation response of the acute gout attack (4). Previous studies have indicated that IL-1 β release is closely followed by neu-

trophil influx in acute gout (3). The dissociation between IL-1 β expression and neutrophil influx in the gouty tophus contrasts with acute gout and warrants further investigation.

Tophi are strongly associated with joint and bone damage in chronic gout (9). The mechanisms of this matrix damage are unclear. It seems unlikely that local pressure by the intraarticular tophus is sufficient to cause such matrix damage. Local production of matrix metalloproteases and tumor necrosis factor α within the tophus may contribute to the development of joint damage (11). The presence of osteoclast-like cells within the tophus may also lead to bone erosion (12). The high expression of IL-1 β within the tophus may coordinate the matrix damage in this disease, through modulation of osteoclastogenesis and induction of matrix-degrading enzymes by stromal cells (29).

The finding that IL-1 β and TGF β 1 expression is present within the same lesion is also noteworthy. These results contrast with those of previous studies using in vitro models of acute gout, which showed that macrophage expression of these cytokines is disconnected and depends on the maturation state of the macrophage (6). It is conceivable that within a complex structure such as the tophus, both proinflammatory and antiinflammatory mediators have parallel biologic effects. In addition to its antiinflammatory role in acute gout, TGF β 1 has been

implicated in tissue remodeling, angiogenesis, and fibrosis in granulomatous disease (30). Thus, this cytokine may contribute to development of the outer fibrovascular zone during tophus formation.

In the current study, we analyzed the cellular architecture of gouty tophi in human patients, using a cross-sectional study design, and raised a number of interesting research questions. This study was not able to analyze the interactions between MSU crystals and the cells within the corona zone, since residual crystals were dissolved during the dewaxing and rehydration stage of the immunohistochemistry protocol. Analysis of these interactions, particularly cytokine production, using other techniques will be of great interest in future studies. Furthermore, it is unclear whether the cells identified within the lesion play a direct role or are bystanders in the initiation and coordination of tophus development. Not all patients develop tophi, even though intraarticular MSU crystals can be detected in almost all previously inflamed joints in patients with untreated gout (31). It is likely that the local burden of MSU crystals does play an important role in tophus formation. However, our data suggest that the host response to intraarticular MSU crystals may also contribute to the development of these lesions.

Longitudinal analysis of tophus formation is currently limited by the lack of adequate models of chronic gout and by the difficulty in obtaining serial samples of human tophi. Although sequential analysis using the air-pouch or peritonitis model of gout has provided insights into the mechanisms of acute gout, such models are not currently used for studying chronic gout and tophus development (18,19,32). Development and validation of an *in vivo* model with which to study tophus formation and the chronic inflammatory response to MSU crystals are now required to determine the host responses that directly contribute to the development of the gouty tophus.

ACKNOWLEDGMENTS

We wish to acknowledge Dr. Alan King, Dr. Michael Dray, and Sharita Meharry who assisted with sample collection and processing. We thank Vivian Ward for assistance with medical illustration. We are grateful to Professor John Highton for critical review of the manuscript.

AUTHOR CONTRIBUTIONS

All authors were involved in drafting the article or revising it critically for important intellectual content, and all authors approved the final version to be published. Dr. Dalbeth had full access to all of

the data in the study and takes responsibility for the integrity of the data and the accuracy of the data analysis.

Study conception and design. Dalbeth, Pool, Callon, McQueen, Cornish.

Acquisition of data. Dalbeth, Pool, Smith, Callon.

Analysis and interpretation of data. Dalbeth, Pool, Gamble, Smith, Callon.

REFERENCES

- Schumacher HR. Pathology of the synovial membrane in gout. Light and electron microscopic studies: interpretation of crystals in electron micrographs. *Arthritis Rheum* 1975;18 Suppl:771–82.
- Dalbeth N, Haskard DO. Mechanisms of inflammation in gout. *Rheumatology (Oxford)* 2005;44:1090–6.
- Martinon F, Petrilli V, Mayor A, Tardivel A, Tschopp J. Gout-associated uric acid crystals activate the NALP3 inflammasome. *Nature* 2006;440:237–41.
- Chen CJ, Shi Y, Hearn A, Fitzgerald K, Golenbock D, Reed G, et al. MyD88-dependent IL-1 receptor signaling is essential for gouty inflammation stimulated by monosodium urate crystals. *J Clin Invest* 2006;116:2262–71.
- Liote F, Prudhommeaux F, Schiltz C, Champy R, Herbelin A, Ortiz-Bravo E, et al. Inhibition and prevention of monosodium urate monohydrate crystal-induced acute inflammation *in vivo* by transforming growth factor β 1. *Arthritis Rheum* 1996;39:1192–8.
- Yagnik DR, Evans BJ, Florey O, Mason JC, Landis RC, Haskard DO. Macrophage release of transforming growth factor β 1 during resolution of monosodium urate monohydrate crystal-induced inflammation. *Arthritis Rheum* 2004;50:2273–80.
- Yagnik DR, Hillyer P, Marshall D, Smythe CD, Krausz T, Haskard DO, et al. Noninflammatory phagocytosis of monosodium urate monohydrate crystals by mouse macrophages: implications for the control of joint inflammation in gout. *Arthritis Rheum* 2000;43:1779–89.
- Dalbeth N, Collis J, Gregory K, Clark B, Robinson E, McQueen FM. Tophaceous joint disease strongly predicts hand function in patients with gout. *Rheumatology (Oxford)* 2007;46:1804–7.
- Dalbeth N, Clark B, Gregory K, Gamble G, Sheehan T, Doyle A, et al. Mechanisms of bone erosion in gout: a quantitative analysis using plain radiography and computed tomography. *Ann Rheum Dis* 2009;68:1290–5.
- Palmer DG, Hogg N, Denholm I, Allen CA, Highton J, Hessian PA. Comparison of phenotype expression by mononuclear phagocytes within subcutaneous gouty tophi and rheumatoid nodules. *Rheumatol Int* 1987;7:187–93.
- Schweyer S, Hemmerlein B, Radzun HJ, Fayyazi A. Continuous recruitment, co-expression of tumour necrosis factor- α and matrix metalloproteinases, and apoptosis of macrophages in gout tophi. *Virchows Arch* 2000;437:534–9.
- Dalbeth N, Smith T, Nicolson B, Clark B, Callon K, Naot D, et al. Enhanced osteoclastogenesis in patients with tophaceous gout: urate crystals promote osteoclast development through interactions with stromal cells. *Arthritis Rheum* 2008;58:1854–65.
- Martin WJ, Walton M, Harper J. Resident macrophages initiating and driving inflammation in a monosodium urate monohydrate crystal-induced murine peritoneal model of acute gout. *Arthritis Rheum* 2009;60:281–9.
- Landis RC, Yagnik DR, Florey O, Philippidis P, Emons V, Mason JC, et al. Safe disposal of inflammatory monosodium urate monohydrate crystals by differentiated macrophages. *Arthritis Rheum* 2002;46:3026–33.
- Juffermans NP, Florquin S, Camoglio L, Verbon A, Kolk AH, Speelman P, et al. Interleukin-1 signaling is essential for host defense during murine pulmonary tuberculosis. *J Infect Dis* 2000;182:902–8.

16. Hessian PA, Highton J, Kean A, Sun CK, Chin M. Cytokine profile of the rheumatoid nodule suggests that it is a Th1 granuloma. *Arthritis Rheum* 2003;48:334–8.
17. Curry AJ, Kaye PM. Recombinant interleukin-1 α augments granuloma formation and cytokine production but not parasite clearance in mice infected with *Leishmania donovani*. *Infect Immun* 1992;60:4422–6.
18. Getting SJ, Flower RJ, Parente L, de Medicis R, Lussier A, Wolitzky BA, et al. Molecular determinants of monosodium urate crystal-induced murine peritonitis: a role for endogenous mast cells and a distinct requirement for endothelial-derived selectins. *J Pharmacol Exp Ther* 1997;283:123–30.
19. Schiltz C, Liote F, Prudhommeaux F, Meunier A, Champy R, Callebert J, et al. Monosodium urate monohydrate crystal-induced inflammation in vivo: quantitative histomorphometric analysis of cellular events. *Arthritis Rheum* 2002;46:1643–50.
20. Lee DM, Friend DS, Gurish MF, Benoist C, Mathis D, Brenner MB. Mast cells: a cellular link between autoantibodies and inflammatory arthritis. *Science* 2002;297:1689–92.
21. Nigrovic PA, Lee DM. Mast cells in inflammatory arthritis. *Arthritis Res Ther* 2005;7:1–11.
22. Hasselbacher P, Schumacher HR. Immunoglobulin in tophi and on the surface of monosodium urate crystals. *Arthritis Rheum* 1978;21:353–61.
23. Bardin T, Varghese Cherian P, Schumacher HR. Immunoglobulins on the surface of monosodium urate crystals: an immunoelectron microscopic study. *J Rheumatol* 1984;11:339–41.
24. Kozin F, Ginsberg MH, Skosey JL. Polymorphonuclear leukocyte responses to monosodium urate crystals: modification by adsorbed serum proteins. *J Rheumatol* 1979;6:519–26.
25. Kanevets U, Sharma K, Dresser K, Shi Y. A role of IgM antibodies in monosodium urate crystal formation and associated adjuvanticity. *J Immunol* 2009;182:1912–8.
26. McGill NW, Dieppe PA. The role of serum and synovial fluid components in the promotion of urate crystal formation. *J Rheumatol* 1991;18:1042–5.
27. Takemura S, Braun A, Crowson C, Kurtin PJ, Cofield RH, O'Fallon WM, et al. Lymphoid neogenesis in rheumatoid synovitis. *J Immunol* 2001;167:1072–80.
28. Dalbeth N, Smith T, Gray S, Doyle A, Antill P, Lobo M, et al. Cellular characterisation of magnetic resonance imaging bone oedema in rheumatoid arthritis: implications for pathogenesis of erosive disease. *Ann Rheum Dis* 2009;68:279–82.
29. Zwerina J, Redlich K, Polzer K, Joosten L, Kronke G, Distler J, et al. TNF-induced structural joint damage is mediated by IL-1. *Proc Natl Acad Sci U S A* 2007;104:11742–7.
30. Roberts AB, Sporn MB, Assoian RK, Smith JM, Roche NS, Wakefield LM, et al. Transforming growth factor type β : rapid induction of fibrosis and angiogenesis in vivo and stimulation of collagen formation in vitro. *Proc Natl Acad Sci U S A* 1986;83:4167–71.
31. Pascual E. Persistence of monosodium urate crystals and low-grade inflammation in the synovial fluid of patients with untreated gout. *Arthritis Rheum* 1991;34:141–5.
32. Pessler F, Mayer CT, Jung SM, Behrens EM, Dai L, Menetski JP, et al. Identification of novel monosodium urate crystal regulated mRNAs by transcript profiling of dissected murine air pouch membranes. *Arthritis Res Ther* 2008;10:R64.